V European Conference on Computational Fluid Dynamics
ECCOMAS CFD 2010
J. C. F. Pereira and A. Sequeira (Eds)
Lisbon, Portugal, 14–17 June 2010

OPTIMAL CFD ANALYSIS FOR LOW POWER SYSTEMS

Simao. M.[*]; Ramos. H.[†]

Instituto Superior Técnico
Av. Rovisco Pais, 1049-001 Lisboa Portugal
[*]MSc in Civil Engineering
e-mail: 85simz@gmail.com

Instituto Superior Técnico
Av. Rovisco Pais, 1049-001 Lisboa Portugal
†Professor, Civil Engineering Department
e-mail: hr@civil.ist.utl.pt

Key words: Low power turbines, Hydrodynamic behaviour, CFD, Performance curves.

Abstract. *This work aims to develop optimization analyses of new turbine hydraulic design in a cost-effective solution for possible implementation in water supply systems (WSS) or in other pressurized water pipe infra-structures. In the first stage of this research, a new methodology is presented based on a theoretical technical-economic analysis. To determine the correlation between the flow velocity and pressure fields, the k-ε model, is used in this research. Many turbines are evaluated (i.e., positive displacement (PD), pump as turbine (PAT), propeller with volute at inlet and a tubular propeller with five blades) and sensitivity analyses, to the best configurations, as well as comparisons between performance curves. The analysis are carried out based on non-dimensional parameters (i.e., discharge and head number and efficiency) in order to be possible to make comparisons between the turbomachines.*
Detailed analyses for alternative typical volumetric energy converters are developed on the basis on mathematical and physical fundamentals, as well as on computational fluid dynamics (CFD) associated to the interaction between the flow conditions and the system operation.

1. INTRODUCTION

As a promising cost-effective energy solution, rotor-dynamic turbo-machines are being under investigation, based on the basic principles associated to a pump operating as a turbine, as well as a non-conventional axial propeller device, as an especially suitable solution for rural or isolated zones or even for grid connected systems [3].

This study deals with four innovative solutions as feasible answer to solve the energy problems with a pressurized integrated-solution for water supply systems or in small available heads in rivers. These solutions can provide a cost-effective alternative to actual turbines especially appropriate for micro hydropower generation due to its simplicity and designer. The numerical simulations help to investigate different types of configurations and parameters that cannot (or not easily) be adopted or measured experimentally. These hydro-machines are focused on small power values since, for higher power values, different turbines suitable for different system characteristics are available on the market. Possible solutions of efficient low-power hydro-machines are not still available on the market. However there are pumps operating as turbines (i.e., pumps operating in reverse mode, referred as PAT) and an open field for new converters.

The Hydrodynamic fluid mechanical analysis requires the use of complex advanced models (CFD) for the grid creation as well as for the hydrodynamic simulation, which apply Navier-Stokes equations by using mathematical models of conservation laws, for the study of the flow behavior. Taking the flow as a subject of specific turbulence, detailed models are necessary in order to determine the correlation between the flow and the velocity pressure fields such as the k-ε model, used in this research [2].

2. VIABILITY ANALYSIS

In recent years, many techniques have been developed to date, including those of [8], and, more recently, [16], [1], [5-6], [15], [14], and [11-12] underline the use of pumps as turbines to operate as a substitute of conventional turbines, i.e., replacing the expensive classical turbine units.

Due to the large existing market for water pumps, they tend to be less expensive than conventional water turbines. In this analysis, the operational and maintenance costs were not taken into account since these costs have less significance than the investment cost. For a payback period of six years, when compared with a conventional water turbine, the system is only economically cost effective for a power output above 10 kW.

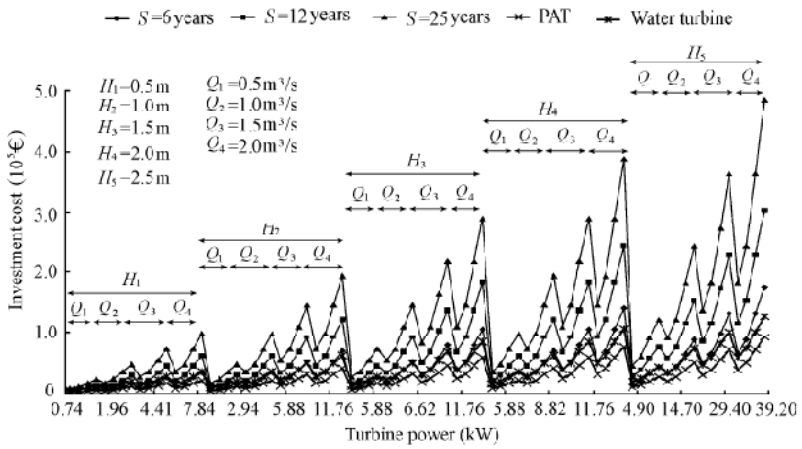

Figure 1 - Investment cost vs turbine power with varying H and Q for different payback periods [3].

With increasing power output, higher initial investments are permitted, since the amount of energy produced and sold to the grid is higher, increasing the project's profits. An increasing trend of cost effectiveness with the increase of payback periods with varying H, Q, and efficiency is shown in Figure 1, in which the efficiencies 30%, 40%, 60%, and 80% correspond to the flow intervals Q1, Q2, Q3, and Q4, respectively [3].

3. CONVERTERS DEVELOPMENT

3.1. Positive displacement turbine

To design the geometry of the positive displacement turbine rotor, it begins to represent two circles, with the aim of having a larger radius greater than 1.5 times the minor radius, such as a larger radius of 10 cm and a minor radius about 6.7 cm. Later it is designed three arches, with equal amplitude, which constituted the rotor, then the enclosure described by the motion of the rotor around a fixed axis (corresponding to the smaller circle). Bounded in the surrounding of the rotor, it is defined two inputs and two outputs with the requirement that each entry and exit coincides with the extreme position of the rotor, that is, when two vertices of the rotor are aligned vertically and symmetrically in relation to the x (Figure 2). The choice to align the entrance and exit to the extreme position of the rotor, allows to isolate fluid from a cavity, thus reducing losses during the passage of flow, and leakage. According to Figure 2 is possible to distinguish the two inputs and two outputs of the flow, which are diametrically symmetrical to plans x and y. Upon completion the geometry of the PD turbine, a mesh creation is made, processing the volumes of the project to model "workbench". In developing the mesh and the definition of boundary conditions of the device, it is necessary to identify the point of rotation of the rotor, since as the rotor moves, this point changes due to the eccentricity of rotation. Because of this difficulty, several movements of the rotor are drawn, identifying the point of tangency between the rotor and the fixed axis.

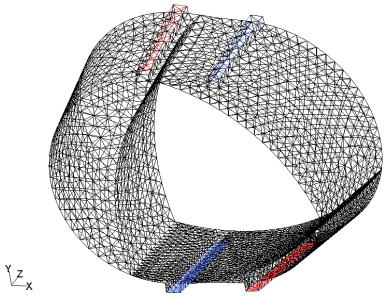

Figure 2 - Mesh generated for the positive displacement turbine.

3.2. Pump as turbine

The mesh generated for this machine requires initially a mesh creation on the faces of the runner followed by a distribution function. The interval value adopted in the face and the distribution function applied to the volume of the structure, is quite different from the values applied to other turbines, since the complexity of the design requires a more refined mesh near the runner. From this function it is created a mesh in the volume set, more refined in the blades, due to its thinness, spreading to other areas surrounding the turbine to complete all settings and remaining space (Figure 3).

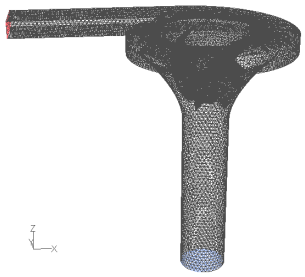

Figure 3 - Mesh defined for PAT.

Regarding the boundary conditions, was considered the boundaries upstream the volute (shown in red in Figure 3), downstream of the draft tube (shown in blue on the same figure), the solid surfaces of all sides of the runner and all remaining faces surrounding the total volume. The separation of the boundary runner, allows FLUENT model to implement only one rotation at the runner without influencing the entire volume.

3.3. Propeller with volute

To determine the shape of the runner blade profile, it is important to starting from the available boundary condition of head and discharge existed in the facility [13] (1,75 meters and 75 l/s), which clearly point towards an axial flow turbine design. Since the most popular design procedure for axial flow turbo-machines is undoubtedly the free vortex design, it should be considered for the runner development. In order to determine the blade shape it is important to fix the operating speed and the tip runner diameter, in addition to the head and flow data. The blade shape comprises of determining the short length, inlet and exit blade angles at all the radial sections beginning from the hub to the tip. The number of blades is another parameter that needed to be chosen and fixed [13].
To validate the theory of the free vortex, the project of this propeller is characterized with several experimental tests, in each step changed the geometry and hence its performance. The origin of the free vortex is represented mainly by the angular momentum law conservation. The primary conditions as the irrotacional flow and axial constant velocity need to satisfy this law. Equation (1) represents the final form of the free vortex law [13].

$$c_u \cdot r = \text{constante} \tag{1}$$

This product of the tangential velocity of the radius is constant throughout the region of entry and exit of the blade and it can be given by the following expression,

$$[c_u \cdot r]_{inlet} = K_{inlet} \quad \text{e} \quad [c_u \cdot r]_{exit} = K_{exit} \tag{2}$$

The constants of Equation (2) are not equal in magnitude. In general, an axial flow turbine constant (K_{inlet}) at the entrance depends on the head. To maximize the energy transfer, the tangential velocity output is taken as zero ($[c_u \cdot r]_{exit} = 0$) along the profile blade outlet and therefore $K_{exit} = 0$. In addition, the radius of the axial turbine increases continuously from the axis of the blade to the periphery, causing the component cu to decrease (Figure 4).

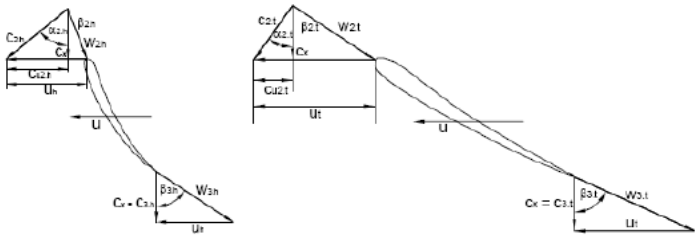

Figure 4 - Speed triangles of entry and exit in the hub and the tip of the blade [13].

The optimization results show a success in the development of this mechanism under certain conditions. The optimization corresponds to a power of 810 W, for a head of 1.75 m, speed of 900 rpm (N_{sqt} = 138 rpm (m, m^3/s)) and a discharge of 64 l/s with an optimum efficiency of 74%. The best angles of the blades which have led to income comprises are: α_1 = 65º and α_2 = 74º in the tip and α1 = 50º and α2 = 55º along the axis.

According to the defined angles for the blades, the first step to do is to trace along the axis and its periphery the development of each blade, by adopting a thickness of 1mm. Established the geometry of the turbine, it is used the CFX model to focus the theoretical axis of the propeller and the mesh is generated on the faces of the propeller, with an interval of one unit between elements (Figure 5).

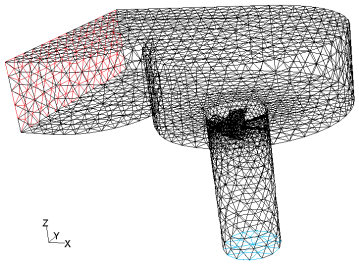

Figure 5 - Mesh generated for the propeller with volute.

In figure above, the boundary conditions corresponds to the face located upstream of the volute (area indicated in red), the downstream face of the draft tube (face shown in blue), all prominent faces of the propeller, classified as wall, and finally all other faces surrounding the volume control, also selected as wall.

3.4. Tubular propeller

The design of the tubular propeller is broken down into a series of solid independent of each other in order to facilitate and promote the creation of separate solutions. As an option is drawn the axis which connects the generator and then the shape of the blade, consisting of angles of entry and exit in the hub and the tip. For the angles of the blades it is necessary mathematical calculations based on speed triangles at inlet and outlet of each blade. Based on these information, each blade orientation gives rise to a new configuration, in order to choose the best solution. It is a lengthy process that requires special care and sensitivity analysis to various parameters.
After the definition of the blade, the propeller is represented, according to the angles referenced, with driven blades based on a rotational speed with a certain direction (equal to the clockwise or negative direction). As the rotational speed depends on how the flow goes through the blades, the rotation value was opted by corresponding to a negative flow direction perpendicular to the face of the shaft rotation with downward (top to bottom).

According to Figure 6, the flow enters on the left side of the pipe goes through the blades and exits vertically.

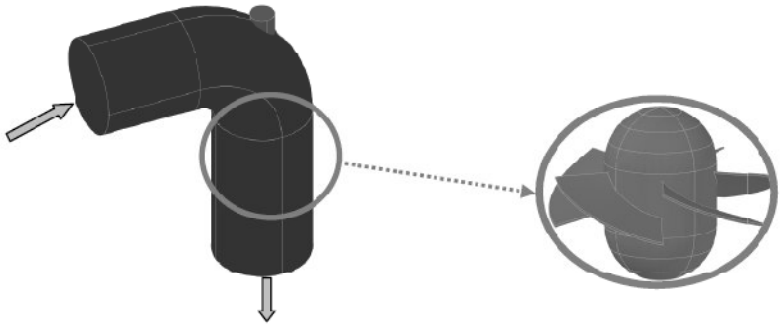

Figure 6 – Scheme of the tubular propeller.

It is important to create a thickness as minimal as possible for the blades in order to avoid interference with the flow, causing additional losses that might constrain its effectiveness. The thickness of 1mm is considered for physical reasons and limitations of mesh generation [4]. To establish the boundary conditions, it is identified the face where the flow enters, indicated in blue (Figure 7), and the face through which exits shown in red in the same figure, and the remaining solid faces considered individually as walls.

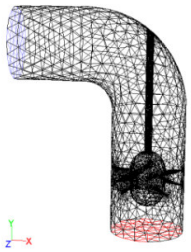

Figure 7 - Mesh created for the tubular propeller with five blades.

For the mesh occupied by the flow, it is created an automatic distribution function from faces, previously spotted. The faces chosen for this purpose are more restricted in places where the mesh is difficult to create, which usually coincides with volumes rather small.

4. CFD RESULTS

4.1. Positive Displacement Turbine

This study proceeds to an analysis of sensitivity to various parameters. Once this process always presupposes the existence of two different magnitudes, in addition to the pressure data it is necessary to specify the value for the rotational speed of the rotor, which in this instance has a positive direction. The study includes analysis of different parameters which allows the observation of which head and rotation speed leads better efficiencies, and what range of discharge and head are more appropriate to intended operation. Thus, the layout of the curves that is associated to the behaviour of this turbine are theoretical, based on 3D hydrodynamic modelling to analyse the interaction between the flow and mechanical components of the turbine.

According to Figure 8, it can be observed the response of the turbine to the variations of some parameters, allowing identifying the best operating point, which corresponds to a rotation speed of 200 rpm (N = 191 rpm, N_{sqt} = 12 rpm (m, m^3/s)).

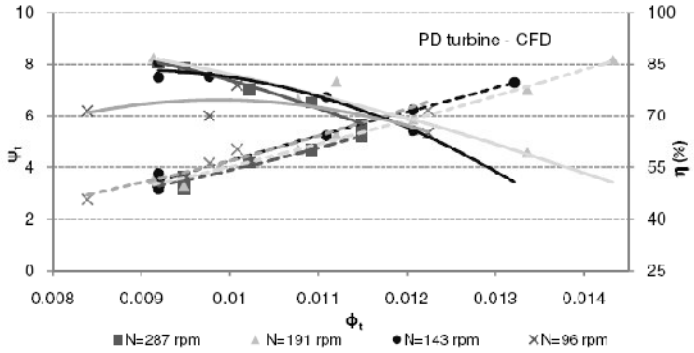

Figure 8 - Variation of efficiency and the head number versus discharge number for different rotational speeds.

For this speed, it is shown the behaviour of the flow inside the turbine to a head of 3 meters and a discharge of approximately 21 l/s, through Figures 9 to 11.

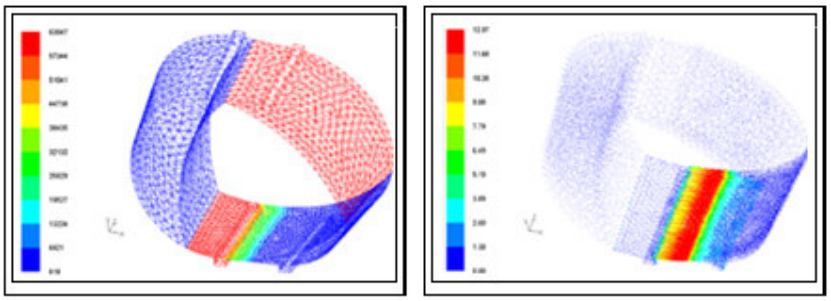

(a) Total pressure (Pa) (b) Velocity vectors (m/s)

Figure 9 - Turbine positive displacement: variation of pressure and flow velocity.

In general, the flow velocity in the interior cavities is low, showing a small leak at the junction between the rotor and the enclosure, Figure 9 (b). For the analysis conditions it is shown that, in the area where the position of the rotor is close to the enclosure, the flow velocity is high, being that area associated with a higher shear stress and turbulence intensity (Figure 10).

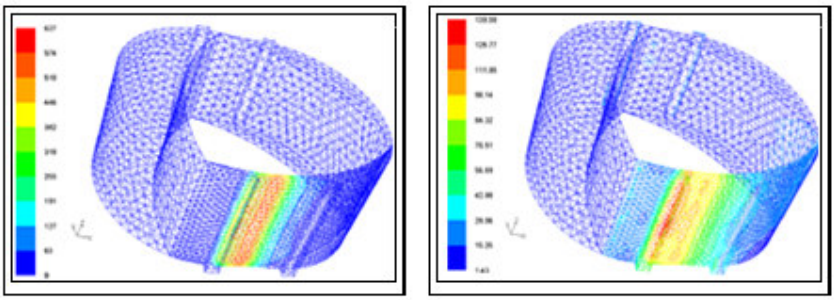

(a) Wall shear stress (Pa) (b) Turbulence intensity (%)

Figure 10 - Turbine positive displacement: variation of wall shear stress and turbulence intensity.

From the pathlines of flow particles it can be identified, in more detail, the behaviour of

the fluid inside the machine.

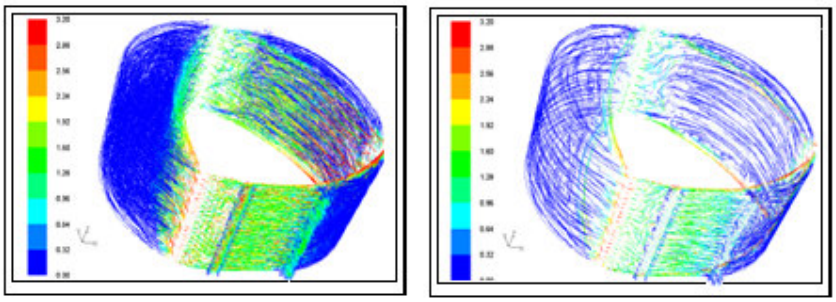

(a) Interior pathlines (m/s) (b) Pathlines near the wall (m/s)

Figure 11 - Turbine positive displacement: Pathlines inside the closure and near the solid boundary (rotor and casing).

In Figure 11 (a) and (b), there are pathlines both inside the cavities as the border delineated by the solid rotor and casing (epicycloid). It is noticed that the existence of narrows passage between the rotor and the outer wall induces a certain shear stress.

4.2. Pump as turbine

As the objective to achieve appropriate solutions, all work has to be developed based on a good quality mesh, in order to be able to model non-conventional effects like turbulence in certain areas of the runner. After the mesh generation and application of the geometry model, the hydrodynamic simulation allows to identify the best efficiency point of the PAT, that corresponds to a runner speed of 100 rad/s or 1000 rpm (N_{sqt} = 32 rpm (m, m^3/s)), a turbine flow of 0.044 m^3/s, and a head about 11.4 m [7]. For these data it is obtained representations of velocity, pressure, turbulence, shear stress and pathlines. In Figure 12 are presented the characteristics curves expressed as a variation head coefficient and efficiency in terms of discharge coefficient for three values of runner speed (N = 800, 1000 and 1500 rpm). The efficiencies for this rotational speed range are above 40% with very promising values in terms of possible real application.

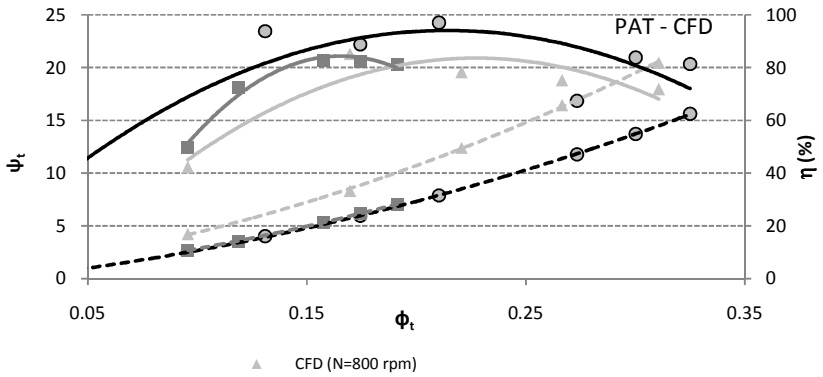

Figure 12 - Evolution of the efficiency and head number vs discharge number for different rotational speeds..

Figures 13 and 14 show the evolution of pressure variation and the velocity vectors along the PAT. According to the values it is identified critical areas that will influence the

efficiency losses under certain operating conditions.

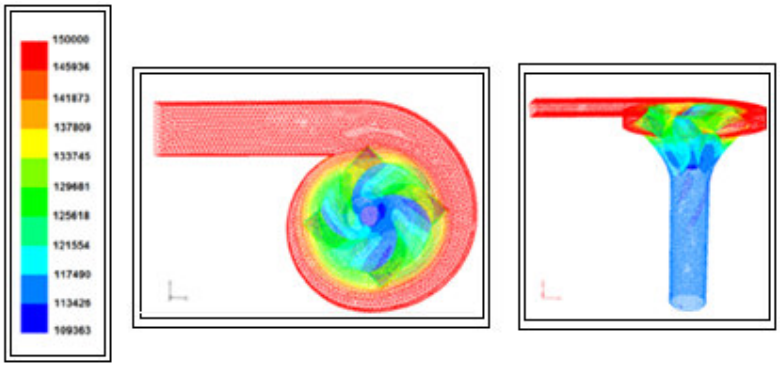

Figure 13 –Total pressure (Pa).

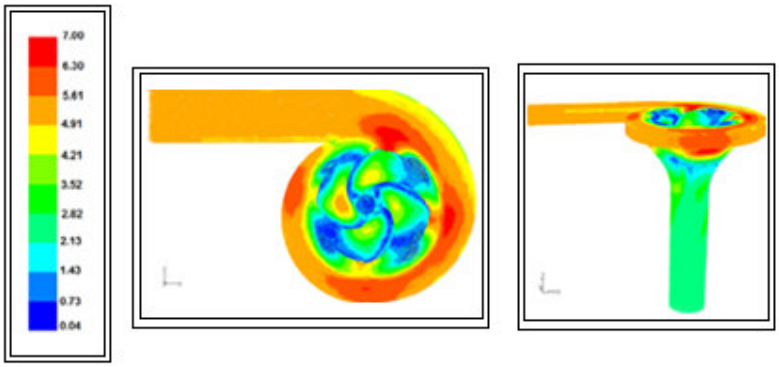

Figure 14 –Flow velocity vectors (m/s).

The velocity vectors are of the highest values along the periphery of the blades, since the flow enter the volute diagonally changing its direction following the movement of the runner, leaving it axially. Due to the centrifugal force on the volute, this induces concentration effects of velocity vectors in the periphery areas (Figures 13 and 14). Figure 15 shows the development of turbulence in critical zones.

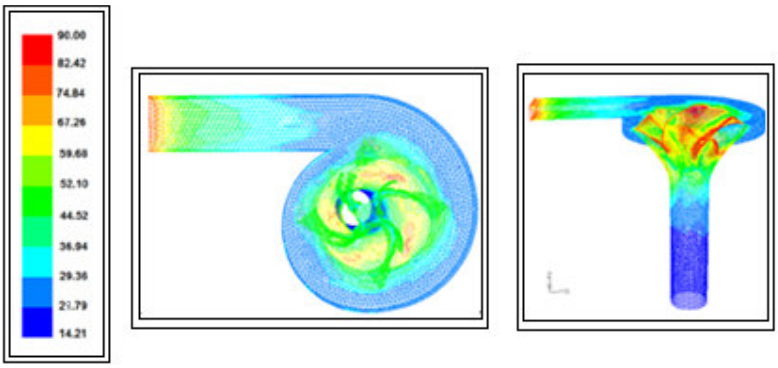

Figure 15 –Turbulence intensity (%).

Figure 16 shows critical areas where the shear stress assumes values more significant and which are primarily near the runner.

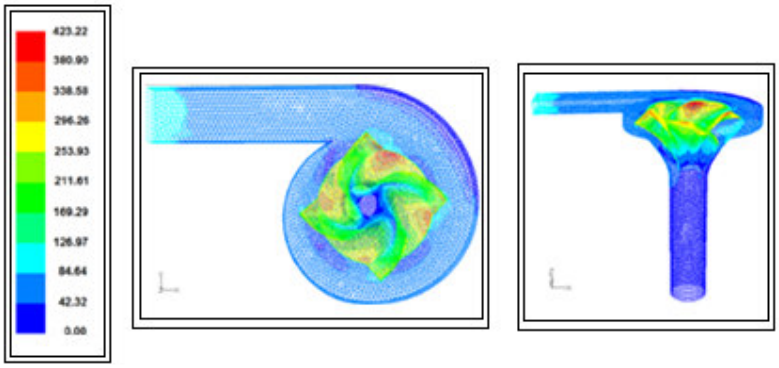

Figure 16 – Wall shear stress (Pa).

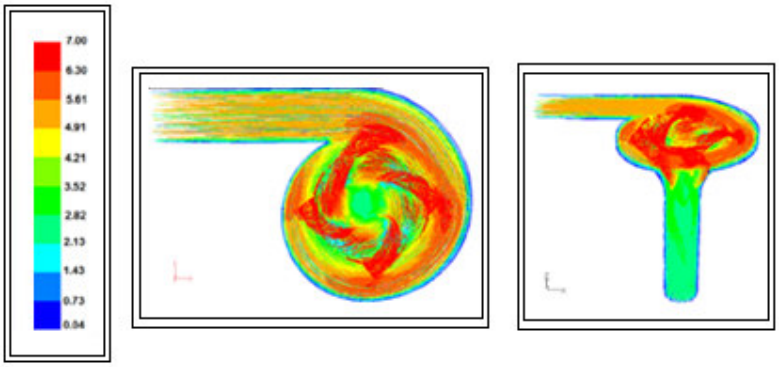

Figure 17 –Streamlines along the volute and the PAT (m/s).

Figure 17 displays the pathlines along the PAT, where the velocity vectors assume greater significance mainly in the area of the runner.

4.3. Propeller with volute

In order to predict possible applications in field, some CFDs simulations were developed from the calibration based on experimental tests.

During the analysis of fluid mechanics (CFD), the interaction between the flow and boundary conditions were analysed. Imposing a fixed speed and providing the value of pressure and discharge, a range of values for each speed were obtained, introducing in every group of iterations a different value for the runner speed (Figure 18).

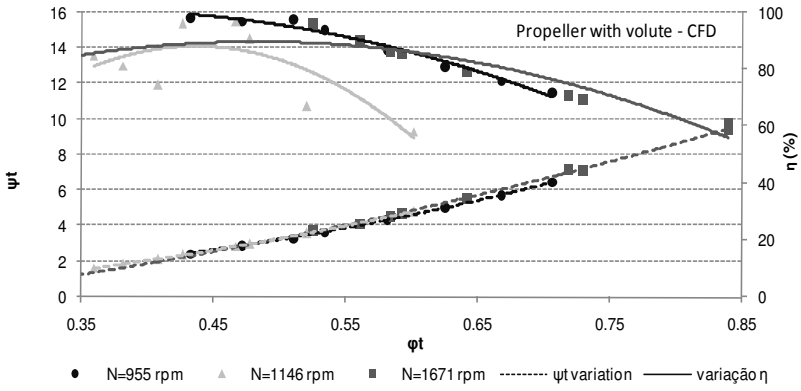

Figure 18 – Variation of efficiency and head number vs discharge number, for different rotational speeds.

These values, therefore, cover a certain range near the optimum value of efficiency. As a result for the dimensions of this machine, a speed of 955 rpm (N_{sqt} = 112 rpm (m, m^3/s)) was reached, leading to the better efficiency. For this optimal solution graphics about pressure, wall shear stress and turbulence intensity for a selected discharge of 55 l/s and head of 2.53 m were made. In Figure 19 (a) can be observed the effect of the volute configuration in the velocity flow at the entrance of the runner, leading to an axial motion. This result is due to the configuration of volute, which doesn't transmit large changes in the circulation of fluid. In Figure 19 (b), the pressure is maximum when the speed is minimal, caused by the irrotacional motion upstream the volute. Once the flow passes through the propeller runner, the pressure keeps high values as well as the flow velocities, which means that the pressure and speed are high due to the rotational motion in the runner. Then, the flow leaves the propeller in a rotational motion, decreasing its pressure and speed values as it loses contact with the runner.

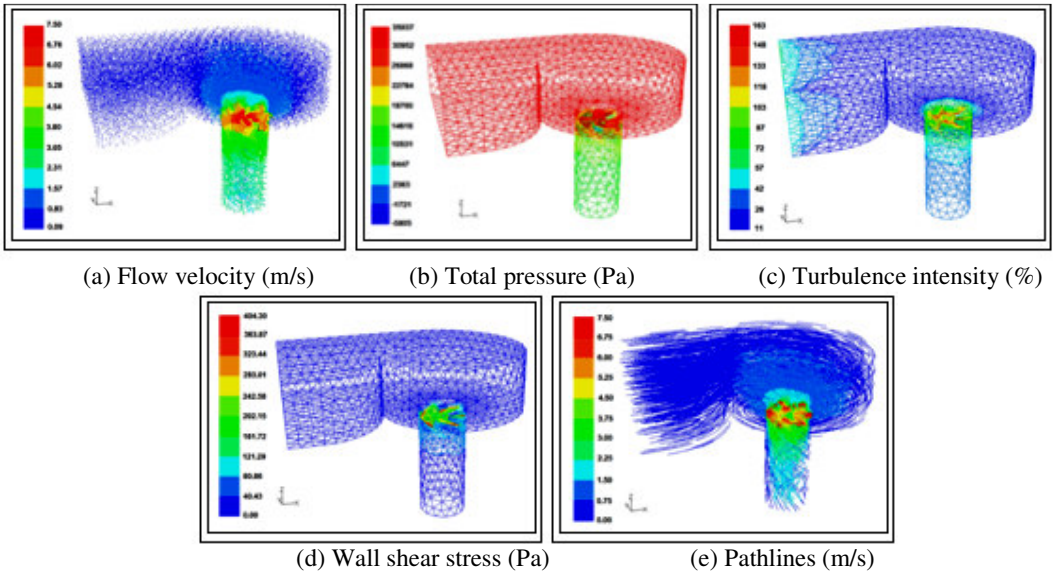

(a) Flow velocity (m/s) (b) Total pressure (Pa) (c) Turbulence intensity (%)

(d) Wall shear stress (Pa) (e) Pathlines (m/s)

Figure 19 - Fluid performance inside the propeller with volute.

From the variation of turbulence intensity presented in Figure 19 (c), it is noticed greater disturbance in the flow, which earns more emphasis on the propeller blades. This distinction of values results from the contribution of the rotation of the propeller in the flow, causing changes in the direction of the velocity field. In Figure 19 (d), is located the area where there is greater resistance in the flow, which coincides with the location of the impeller. This resistance is in the runner and the proximity of the blades with the outer border, which causes significant friction during the movement of the fluid in that region. Figure 19 (e) shows in more detail the effect that the volute and the flow in the runner. Here is evident the better transition from axial movement, upstream the runner, to radial motion with rotation movement, downstream of the turbine.

4.4. Tubular Propeller

The efficiency is estimated by assessing values by the CFD model which leads to the conclusion that for a speed of 1337 rpm (N_{sqt} = 69 rpm (m, m^3/s)), a discharge of 13 l/s and a head of 2.85 m, the turbine efficiency obtained by the simulation is good (Figure 20).

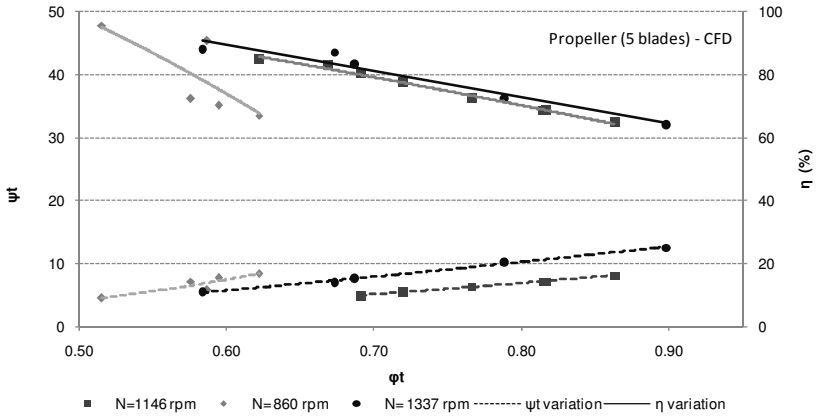

Figure 20 – Variation of efficiency and head number vs discharge number, for different rotational speeds.

Given the characteristic curves of this machine and established the BEP, the diagrams of velocity, pressure, turbulence, shear stress, and pathlines of flow particles are presented being possible to understand the behaviour of the system. Analyzing Figure 21 (a), the flow velocity has little variation from the entrance of the tubular turbine, where there are some local regions near the turbine shaft and the curve. In the impeller the flow is conditioned with some changes in the direction of its trajectory.

Comparing Figure 21 (a) and (b) the flow presents a low velocity, with high pressure values in that region. This is explained by the irrotacional flow at the entry. However, when entering into the impeller rotation field, the flow becomes rotational failing to maintain a constant load. This condition requires an increase of flow velocity and an increase in pressure. In the diagram of pressures, there is a reduction in the pressure in the lower region of the propeller, caused by the effect of separation of the outflow.

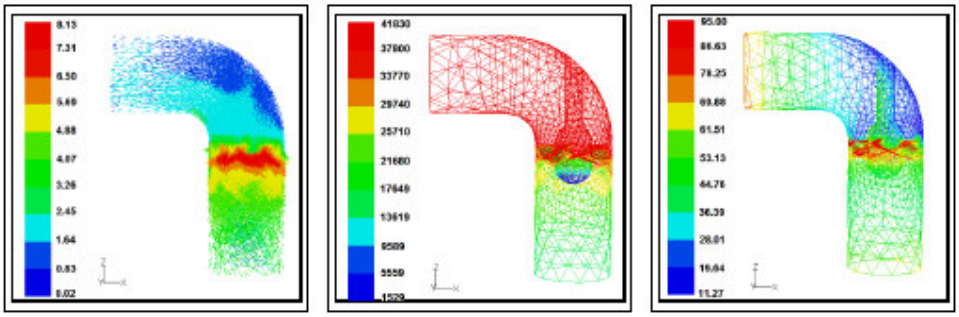

(a) Flow velocity (m/s) (b) Total pressure (Pa) (c) Turbulence intensity (%)

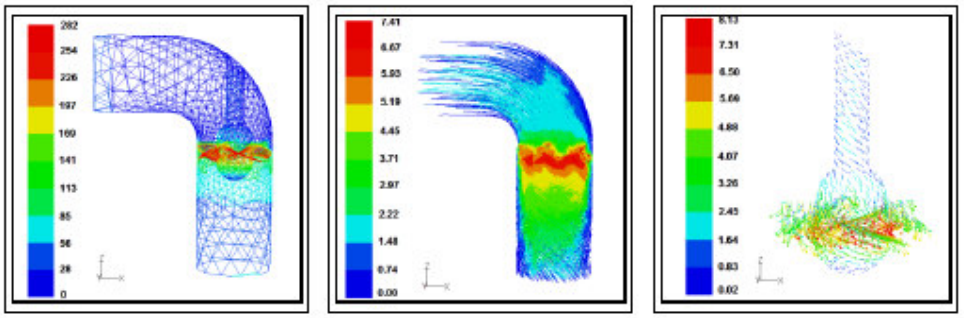

(d) Wall shear stress (Pa) (e) Pathlines (m/s) (f) Velocity vectors (m/s)

Figure 21 – Tubular propeller with five blades.

According to Figure 21 (c), it is observed the turbulence along the tubular propeller turbine. In Figure 21 (d), the shear stress is higher near the periphery of the blades, where the flow exit the blade with rotation as it can be observed in Figure 21 (e) conferring some significant resistance to the flow. In Figure 21 (f) it is possible to visualize the velocity vectors along the propeller wall [10].

5. CONCLUSIONS

These results show that CFD models are very useful to simulate the hydrodynamic flow inside of each engine. It constituted a vital part in the design and development of new turbines, enabling virtual prototypes motion and simulating their performance as well as optimizing some components (e.g. bulb, thickness and position and blades configuration). Its use reduces the need for testing and analysis of other less common scenarios, after an appropriate calibration in physical prototypes under certain operating conditions. These new design solutions are appropriate to hydropower schemes with small head and discharge values, reforming the idea of introducing and develop new converters in order to cover a large range of applications where low power are available, especially in pipe systems.

The most interesting conclusions of this study are to the internal optimization of these new energy engines and the elimination of as much of the expensive additional control systems as possible. This comprised the study of the flow behaviour regarding power, discharge, hydraulic and shear stress effects under different values of head and turbine speeds [4]. These models also allow making some comparisons between CFD and experimental tests, leading to a greater knowledge of interaction between machine geometry and hydraulic characteristics.

ACKNOWLEDGMENTS

To projects HYLOW from 7th Framework Programme (grant nº 212423) and FCT (PTDC/ECM/65731/2006) which contributed to the development of this research work.

REFERENCES

[1] C. Alatorre-frenk, Cost Minimization in Micro-Hydro Systems Using Pumps-as-Turbines. Ph. D. Dissertation. Coventry: University of Warwick. (1994).

[2] Fluent 6.3, User's Guide. USA (2006).

[3] H. M. Ramos, A. Borga, M. Simão, Cost-effective energy production in water pipe

systems: theoretical analysis for new design solutions. *33rd IAHR Congress. Water Engineering for a Sustainable Environment. Managed by EWRI of ASCE on behalf of IAHR*. Vancouver, British Columbia, Canada, August 9-14 (2009).

[4] H. M. Ramos, A. Borga, M. Simão, New design solutions for low-power energy production in water pipe systems. *Water Science and Engineering, 2(4): 69-84, doi:10.3882/j.issn.1674-2370.2009.04.007* (2009).

[5] H. M. Ramos, A. Borga, Pumps as turbines: Unconventional solution to energy production. *Urban Water, 1(3), 261-263. [doi: 10.1016/S1462-0758(00)00016-9]* (1999).

[6] H.M. Ramos, A. Borga, Pumps yielding power. *Dam Engineering, 10(4), 197-217* (2000).

[7] S. Rawal, J. T. Kshirsagar, Numerical Simulation on a Pump Operating in a Turbine Mode. *Proceedings of the Twenty-Third International Pump Users Symposium.* USA, Texas AM University (2007).

[8] K. R. Sharma, Small Hydroelectric Projects: Use of Centrifugal Pumps as Turbines. *Bangalore: Kirloskar Electric Co* (1985).

[10] M. Simão, Hydrodynamic and performance of low power turbines: conception, modelling and experimental tests. Master Thesis. Portugal, Instituto Superior Técnico, (2009).

[11] P. Singh, Establishment of a Test-Rig for Turbine for Micro Hydro and Detailed Testing of a Pump as Turbine, *24-26. New Delhi: Centre for Energy Studies*, Indian Institute of Technology. (2001).

[12] P. Singh, Optimization of the Internal Hydraulic and of System Design in Pumps as Turbines with Field Implementation and Evaluation. Ph.D. Dissertation. Karlsruhe: University of Karlsruhe. (2005).

[13] P. Singh, F. Nestmann, Experimental optimization of a free vortex propeller runner for micro hydro application. *Experimental Thermal and Fluid Science, Volume 33, Issue 6, September 2009, Pages 991-1002, doi:10.1016/j.expthermflusci.2009.04.007*. (2009).

[14] P. Singh, F. Nestmann, S. Caglar, and J.T. Kshirsagar, Hydraulic performance optimization in pumps as turbines. *Pump Users International Forum*. Karlsruhe: VDMA. (2004).

[15] M. Valadas, H.M. Ramos, Use of pumps as turbines in irrigation systems to profit the available energy in irrigation system. *Water Resources Journal, 24(3), 63-76. (in Portuguese), 2003. Water, 1(3), 261-263. [doi: 10.1016/S1462-0758(00)00016-9]* (1999).

[16] A. A. Williams, Pumps as Turbines Used With Induction Generators for Stand-Alone Micro-Hydroelectric Power Plants. Ph.D. Dissertation. Nottingham: Nottingham Trent University (1992).